

July 4, 2018

Top and Bottom Squarks Decays under Cosmological Bounds

L. Selbuz ¹ and Z. Z. Aydin ²

Department of Engineering Physics, Faculty of Engineering, Ankara University,
06100 Tandogan-Ankara, Turkey

Abstract

We investigate the fermionic decays of top squarks $\tilde{t}_{1,2}$ and bottom squarks $\tilde{b}_{1,2}$ in the Minimal Supersymmetric Standard Model with complex parameters M_1 , μ , A_t and A_b . In the analysis we particularly take into account the cosmological bounds imposed by WMAP data. We plot the CP phase dependences of stop and sbottom decay widths.

PACS numbers: 14.80.Ly, 12.60.Jv

1 Introduction

SUSY provides an appealing realization of the Higgs mechanism for mass generation. When SUSY is broken softly, superpartners acquire masses not exceeding 1 TeV. Since these new particles are in the exploration range of the LHC, we have to analyse non-standard Higgs sector extensively in all possible ways [1].

The minimal supersymmetric extension of the Standard Model (MSSM) requires a non-minimal Higgs sector [2] which introduces additional sources of CP-violation beyond the

¹e-mail address: selbuz@eng.ankara.edu.tr

²e-mail address: zzaydin@eng.ankara.edu.tr

economical Kobayashi-Maskawa phase of the SM. The plethora of CP-phases also influences the decays and mixings of B mesons (as well as D and K mesons). The present experiments at BABAR, Tevatron and KEK and the one to start at the LHC will be able to measure various decay channels to determine if there are supersymmetric sources of CP violation. In particular, CP-asymmetry and decay rate of $B \rightarrow X_s \gamma$ form a good testing ground for low-energy supersymmetry with CP violation [3]. These additional sources of CP-violation are welcome to explain the cosmological baryon asymmetry of the universe. In addition to this, the lightest superpartner, i.e. the lightest neutralino $\tilde{\chi}_1^0$ could be an excellent candidate for cold dark matter in the universe.

With the precision experiments by Wilkinson Microwave Anisotropy Probe (WMAP), the relic density of cold dark matter can be constrained to $0.0945 < \Omega_{CDM} h^2 < 0.1287$ at 2σ level [4]. Recently, in the light of this cosmological constraint, an extensive analysis of the neutralino relic density in the presence of CP phases has been given by Bélanger *et al.* [5].

Analyses of the decays of third generation scalar quarks with complex SUSY parameters have been performed by Bartl *et al.* [6]. In the present note we repeat this analysis taking into account the cosmological bound imposed by WMAP. Namely, we study the effect of M_1 and its phase $\varphi_{U(1)}$ on the decay widths of $\tilde{t}_{1,2}$ and $\tilde{b}_{1,2}$. In the numerical calculations, although the SUSY parameters μ , M_1 , M_2 , and A_f are in general complex, we assume that μ , M_2 , A_t and A_b are real, but M_1 and its phase $\varphi_{U(1)}$ take values on the WMAP- allowed bands given in Ref. [5]. These bands also satisfy the EDM bounds [7]. And we evaluate the parameter M_2 via the relation $M_2 = 3/5 |M_1| (\tan \theta_W)^{-2}$. It is very important to insert the WMAP-allowed band in the plane $M_1 - \varphi$ into the numerical calculations instead of taking one fixed M_1 value for all φ -phases, because, for example, on the allowed band for $\mu = 200$ GeV, M_1 starts from 140 GeV for $\varphi = 0$ and increasing monotonously it becomes 165 GeV for $\varphi = \pi$. In Ref. [5] two WMAP-allowed band plots are given, one for $\mu = 200$ GeV and the other for $\mu = 350$ GeV. For both plots the other parameters are fixed to be $\tan \beta = 10$, $m_{H^+} = 1$ TeV, $A_t = 1.2$ TeV, $A_b = 1.2$ TeV, $\varphi_\mu = \varphi_{A_t} = \varphi_{A_b} = 0$.

2 Top and Bottom Squarks Masses, Mixing and Decay Widths

2.1 Masses and mixing in squark sector

The superpartners of the SM fermions with left and right helicity are the left and right sfermions. In the case of top squark (stop) and bottom squark (sbottom) the left and right states are in general mixed. Therefore, the sfermion mass terms of the Lagrangian are described in the basis $(\tilde{q}_L, \tilde{q}_R)$ as

$$\mathcal{L}_M^{\tilde{q}} = -(\tilde{q}_L^\dagger \tilde{q}_R^\dagger) \begin{pmatrix} M_{LL}^2 & M_{LR}^2 \\ M_{RL}^2 & M_{RR}^2 \end{pmatrix} \begin{pmatrix} \tilde{q}_L \\ \tilde{q}_R \end{pmatrix} \quad (2.1)$$

with

$$M_{LL}^2 = M_{\tilde{Q}}^2 + (I_{3L}^q - e_q \sin^2 \theta_W) \cos(2\beta) m_z^2 + m_q^2 \quad (2.2)$$

$$M_{RR}^2 = M_{\tilde{Q}'}^2 + e_q \sin^2 \theta_W \cos(2\beta) m_z^2 + m_q^2 \quad (2.3)$$

$$M_{RL}^2 = (M_{LR}^2)^* = m_q (A_q - \mu^* (\tan \beta)^{-2I_{3L}^q}) \quad (2.4)$$

where m_q , e_q , I_{3L}^q and θ_W are the mass, electric charge, weak isospin of the quark $q=b,t$ and the weak mixing angle, respectively. $\tan \beta = v_2/v_1$ with v_i being the vacuum expectation values of the Higgs fields H_i^0 , $i = 1, 2$. The soft-breaking parameters $M_{\tilde{Q}}$, $M_{\tilde{Q}'} = M_{\tilde{U}}(M_{\tilde{D}})$ for $q=t(b)$, A_b and A_t involved in Eqs. (2.2-2.4) can be evaluated for our numerical calculations using the following relations

$$M_{\tilde{Q}}^2 = \frac{1}{2} \left(m_{t_1}^2 + m_{t_2}^2 \pm \sqrt{(m_{t_2}^2 - m_{t_1}^2)^2 - 4m_t^2 |A_t - \mu^* \cot \beta|^2} \right) - \left(\frac{1}{2} - \frac{2}{3} \sin^2 \theta_W \right) \cos(2\beta) m_z^2 - m_t^2 \quad (2.5)$$

$$M_{\tilde{U}}^2 = \frac{1}{2} \left(m_{t_1}^2 + m_{t_2}^2 \mp \sqrt{(m_{t_2}^2 - m_{t_1}^2)^2 - 4m_t^2 |A_t - \mu^* \cot \beta|^2} \right) - \frac{2}{3} \sin^2 \theta_W \cos(2\beta) m_z^2 - m_t^2 \quad (2.6)$$

and similar ones for $M_{\tilde{Q}}$ and $M_{\tilde{D}}$ by interchanging $t \leftrightarrow b$ in Eqs. (2.5-2.6).

The squark mass eigenstates \tilde{q}_1 and \tilde{q}_2 can be obtained from the weak states \tilde{q}_L and \tilde{q}_R via the \tilde{q} -mixing matrix

$$\mathcal{R}^{\tilde{q}} = \begin{pmatrix} e^{i\varphi_{\tilde{q}}} \cos \theta_{\tilde{q}} & \sin \theta_{\tilde{q}} \\ -\sin \theta_{\tilde{q}} & e^{-i\varphi_{\tilde{q}}} \cos \theta_{\tilde{q}} \end{pmatrix} \quad (2.7)$$

where

$$\varphi_{\tilde{q}} = \arg[M_{RL}^2] = \arg[A_q - \mu^*(\tan \beta)^{-2I_{3L}^q}] \quad (2.8)$$

and

$$\cos \theta_{\tilde{q}} = \frac{-|M_{LR}^2|}{\sqrt{|M_{LR}^2|^2 + (m_{\tilde{q}_1}^2 - M_{LL}^2)^2}}, \quad \sin \theta_{\tilde{q}} = \frac{M_{LL}^2 - m_{\tilde{q}_1}^2}{\sqrt{|M_{LR}^2|^2 + (m_{\tilde{q}_1}^2 - M_{LL}^2)^2}} \quad (2.9)$$

One can easily get the following squark mass eigenvalues by diagonalizing the mass matrix in Eq. (2.1):

$$m_{\tilde{q}_{1,2}}^2 = \frac{1}{2} \left(M_{LL}^2 + M_{RR}^2 \mp \sqrt{(M_{LL}^2 - M_{RR}^2)^2 + 4|M_{LR}^2|^2} \right), \quad m_{\tilde{q}_1} < m_{\tilde{q}_2} \quad (2.10)$$

We might add a comment about the possibility of a flavor mixing, for example, between the second and third squark families. In this case, the sfermion mass matrix in Eq. (2.1) becomes a 4x4 matrix in the basis $(\tilde{c}_L, \tilde{c}_R, \tilde{t}_L, \tilde{t}_R)$. Then one obtains squark mass eigenstates $(\tilde{c}_1, \tilde{c}_2, \tilde{t}_1, \tilde{t}_2)$ from these weak states, and analyzes their decays by utilizing procedures similar to the ones indicated in the text. The problem with flavor violation effects is that their inclusion necessarily correlates B, D and K physics with direct sparticle searches at colliders. Moreover, it has been shown that, with sizeable supersymmetric flavor violation, even the Higgs phenomenology at the LHC correlates with that of the rare processes [8]. In this work we have neglected such effects; however, we emphasize that inclusion of such effects can give important information on mechanism that breaks supersymmetry via decay products of squarks.

2.2 Fermionic decay widths of \tilde{t}_i and \tilde{b}_i

The quark-squark-chargino and quark-squark-neutralino Lagrangians have been first given in Ref. [1]. Here we use them in notations of Ref. [6]:

$$\mathcal{L}_{q\tilde{q}\tilde{\chi}^+} = g\bar{t}(\ell_{ij}^{\tilde{b}}P_R + k_{ij}^{\tilde{b}}P_L)\tilde{\chi}_j^+\tilde{b}_i + g\bar{b}(\ell_{ij}^{\tilde{t}}P_R + k_{ij}^{\tilde{t}}P_L)\tilde{\chi}_j^{+c}\tilde{t}_i + h.c. \quad (2.11)$$

and

$$\mathcal{L}_{q\tilde{q}\tilde{\chi}^0} = g\bar{q}(a_{ik}^{\tilde{q}}P_R + b_{ik}^{\tilde{q}}P_L)\tilde{\chi}_k^0\tilde{q}_i + h.c. \quad (2.12)$$

We also borrow the formulas for the partial decay widths of \tilde{q}_i ($\tilde{q}_i = \tilde{t}_i$ and \tilde{b}_i) into quark-chargino (or neutralino) from Ref. [6]:

$$\Gamma(\tilde{q}_i \rightarrow q' + \tilde{\chi}_k^\pm) = \frac{g^2 \lambda^{1/2}(m_{\tilde{q}_i}^2, m_{q'}^2, m_{\tilde{\chi}_k^\pm}^2)}{16\pi m_{\tilde{q}_i}^3} \times \left[\left(|k_{ik}^{\tilde{q}}|^2 + |\ell_{ik}^{\tilde{q}}|^2 \right) (m_{\tilde{q}_i}^2 - m_{q'}^2 - m_{\tilde{\chi}_k^\pm}^2) - 4 \text{Re}(k_{ik}^{\tilde{q}*} \ell_{ik}^{\tilde{q}}) m_{q'} m_{\tilde{\chi}_k^\pm} \right] \quad (2.13)$$

and

$$\Gamma(\tilde{q}_i \rightarrow q + \tilde{\chi}_k^0) = \frac{g^2 \lambda^{1/2}(m_{\tilde{q}_i}^2, m_q^2, m_{\tilde{\chi}_k^0}^2)}{16\pi m_{\tilde{q}_i}^3} \times \left[\left(|a_{ik}^{\tilde{q}}|^2 + |b_{ik}^{\tilde{q}}|^2 \right) (m_{\tilde{q}_i}^2 - m_q^2 - m_{\tilde{\chi}_k^0}^2) - 4 \text{Re}(a_{ik}^{\tilde{q}*} b_{ik}^{\tilde{q}}) m_q m_{\tilde{\chi}_k^0} \right] \quad (2.14)$$

with $\lambda(x, y, z) = x^2 + y^2 + z^2 - 2(xy + xz + yz)$.

The explicit forms of $\ell_{ik}^{\tilde{q}}$, $k_{ik}^{\tilde{q}}$ and $a_{ik}^{\tilde{q}}$, $b_{ik}^{\tilde{q}}$ can be found in Ref. [6]. We have to point out that although at the loop level the SUSY-QCD corrections could be important, our analysis here are merely at tree level, as can be seen from Eqs. (2.13) and (2.14). In this work we content with tree-level amplitudes as we aim at determining the phase-sensitivities of the decay rates, mainly.

3 Top squark decays

Here we present the dependences of the \tilde{t}_1 and \tilde{t}_2 partial decay widths on $\varphi_{U(1)}$ for $\mu = 200$ GeV and for $\mu = 350$ GeV. We also choose reasonable values for the masses ($m_{\tilde{t}_1}$, $m_{\tilde{t}_2}$, $m_{\tilde{\chi}_1^\pm}$, $m_{\tilde{\chi}_2^\pm}$, $m_{\tilde{\chi}_1^0}$) = (350 GeV, 800 GeV, 180 GeV, 336 GeV, 150 GeV) for $\mu = 200$ GeV and ($m_{\tilde{t}_1}$, $m_{\tilde{t}_2}$, $m_{\tilde{\chi}_1^\pm}$, $m_{\tilde{\chi}_2^\pm}$, $m_{\tilde{\chi}_1^0}$) = (350 GeV, 800 GeV, 340 GeV, 680 GeV, 290 GeV) for $\mu = 350$ GeV.

For both sets of values by calculating the $M_{\tilde{Q}}$ and $M_{\tilde{U}}$ values corresponding to $m_{\tilde{t}_1}$ and $m_{\tilde{t}_2}$, we plot the decay widths for $M_{\tilde{Q}} \geq M_{\tilde{U}}$ and $M_{\tilde{Q}} < M_{\tilde{U}}$, separately. Fig.1(a) and Fig.1(b) show the partial decay widths of the channels $\tilde{t}_1 \rightarrow b\tilde{\chi}_1^+$, $\tilde{t}_1 \rightarrow b\tilde{\chi}_2^+$, $\tilde{t}_1 \rightarrow t\tilde{\chi}_1^0$, $\tilde{t}_2 \rightarrow b\tilde{\chi}_1^+$, $\tilde{t}_2 \rightarrow b\tilde{\chi}_2^+$ and $\tilde{t}_2 \rightarrow t\tilde{\chi}_1^0$ as a function of $\varphi_{U(1)}$ for $\mu = 200$ GeV assuming $M_{\tilde{Q}} > M_{\tilde{U}}$ and $M_{\tilde{Q}} < M_{\tilde{U}}$, respectively. There we see some dependences on $\varphi_{U(1)}$ phase.

In order to see these dependences more pronouncedly, in Figs. 5(a)-(d) ($\tilde{t}_{1,2}$ decays for $\mu = 200$ GeV) and Figs. 6(a)-(d) ($\tilde{t}_{1,2}$ decays for $\mu = 350$ GeV) we plot now separately only those decay channels whose dependences on $\varphi_{U(1)}$ are not clearly seen in Fig.1 and Fig.2. $\Gamma(\tilde{t}_1 \rightarrow t\tilde{\chi}_1^0)$ and $\Gamma(\tilde{t}_1 \rightarrow b\tilde{\chi}_1^+)$ decay widths increase as $\varphi_{U(1)}$ increases from 0 to π , but $\Gamma(\tilde{t}_1 \rightarrow b\tilde{\chi}_2^+)$ width decreases as $\varphi_{U(1)}$ increases. On the other hand, $\Gamma(\tilde{t}_2 \rightarrow t\tilde{\chi}_1^0)$ decrease for both $M_{\tilde{Q}} > M_{\tilde{U}}$ and $M_{\tilde{Q}} < M_{\tilde{U}}$ cases as $\varphi_{U(1)}$ increases; $\Gamma(\tilde{t}_2 \rightarrow b\tilde{\chi}_1^+)$ decreases for $M_{\tilde{Q}} > M_{\tilde{U}}$ but increases for $M_{\tilde{Q}} < M_{\tilde{U}}$ and $\Gamma(\tilde{t}_2 \rightarrow b\tilde{\chi}_2^+)$ increases for $M_{\tilde{Q}} > M_{\tilde{U}}$ but decreases for $M_{\tilde{Q}} < M_{\tilde{U}}$.

The branching ratios for \tilde{t}_2 are roughly $B(\tilde{t}_2 \rightarrow b\tilde{\chi}_1^+) : B(\tilde{t}_2 \rightarrow t\tilde{\chi}_1^0) : B(\tilde{t}_2 \rightarrow b\tilde{\chi}_2^+) \approx 8 : 2 : 1$. This simply reflects both the large phase space and large Yukawa coupling for the decay $\tilde{t}_2 \rightarrow b\tilde{\chi}_1^+$.

Figs. 2(a) and 2(b) show the same partial decay widths for $\mu = 350$ GeV. [See also Figs.6(a)-(d)]. They also reveal the significant dependences on CP-violation phase.

For $\mu = 350$ GeV the WMAP-allowed band [5] takes place in larger M_1 values ($\sim 305 - 325$ GeV) leading to larger chargino and neutralino masses. This naturally leads very small decay widths for $\tilde{t}_1 \rightarrow b\tilde{\chi}_1^+$ and kinematically forbidden $\tilde{t}_1 \rightarrow b\tilde{\chi}_1^0$ and $\tilde{t}_1 \rightarrow b\tilde{\chi}_2^+$. Because of the large \tilde{t}_2 mass, \tilde{t}_2 decay processes are still kinematically allowed as seen in Figs. 2(a)-(b). The decay width of the process $\tilde{t}_2 \rightarrow b\tilde{\chi}_1^+$ is the largest one among the \tilde{t}_2 channels and the branching ratios are $B(\tilde{t}_2 \rightarrow b\tilde{\chi}_1^+) : B(\tilde{t}_2 \rightarrow b\tilde{\chi}_2^+) : B(\tilde{t}_2 \rightarrow t\tilde{\chi}_1^0) \approx 4 : 2 : 0.3$. The decay $\tilde{t}_2 \rightarrow t\tilde{\chi}_1^0$ shows strong phase dependence.

4 Bottom squark decays

We give sbottom decay widths as a function of $\varphi_{U(1)}$ in Figs. 3(a)-(b)(for $\mu = 200$ GeV) and in Figs. 4(a)-(b)(for $\mu = 350$ GeV). [See also Figs. 7(a)-(d) and Figs. 8(a)-(c)]. Here we choose the masses $(m_{\tilde{b}_1}, m_{\tilde{b}_2}, m_{\tilde{\chi}_1^\pm}, m_{\tilde{\chi}_2^\pm}, m_{\tilde{\chi}_1^0}) = (550 \text{ GeV}, 800 \text{ GeV}, 180 \text{ GeV}, 336 \text{ GeV}, 150 \text{ GeV})$ for $\mu = 200$ GeV and $(m_{\tilde{b}_1}, m_{\tilde{b}_2}, m_{\tilde{\chi}_1^\pm}, m_{\tilde{\chi}_2^\pm}, m_{\tilde{\chi}_1^0}) = (550 \text{ GeV}, 800 \text{ GeV}, 340 \text{ GeV}, 680 \text{ GeV}, 290 \text{ GeV})$ for $\mu = 350$ GeV. $\Gamma(\tilde{b}_2 \rightarrow b\tilde{\chi}_1^0)$ is smaller than $\Gamma(\tilde{b}_2 \rightarrow t\tilde{\chi}_i^-)$ in spite of large phase space, because in $\tilde{b}_2 \rightarrow b\tilde{\chi}_1^0$ decay only Y_b coupling enters. The dependences of the phase $\varphi_{U(1)}$ in sbottom decays are similar to those in stop decays.

The branching ratios for \tilde{b}_2 decays are $B(\tilde{b}_2 \rightarrow t\tilde{\chi}_1^-) : B(\tilde{b}_2 \rightarrow t\tilde{\chi}_2^-) : B(\tilde{b}_2 \rightarrow b\tilde{\chi}_1^0) \approx$

10 : 7 : 0.5. While the process $\tilde{b}_2 \rightarrow b\tilde{\chi}_1^0$ is suppressed more than one order its dependence on $\varphi_{U(1)}$ is prominent such that the value of decay width at $\varphi_{U(1)} = 0$ is 2 times larger than that at $\varphi_{U(1)} = \pi$. φ -dependences of the process $\tilde{b}_2 \rightarrow t\tilde{\chi}_1^-$ and $\tilde{b}_2 \rightarrow t\tilde{\chi}_2^-$ can be seen easily in Fig. 3(a).

For $M_{\tilde{Q}} < M_{\tilde{D}}$, $\tilde{b}_1 \rightarrow t\tilde{\chi}_1^-$ decay is about five times larger than $\tilde{b}_2 \rightarrow t\tilde{\chi}_1^-$. The branching ratios for \tilde{b}_1 decays are $B(\tilde{b}_1 \rightarrow t\tilde{\chi}_1^-) : B(\tilde{b}_1 \rightarrow t\tilde{\chi}_2^-) : B(\tilde{b}_1 \rightarrow b\tilde{\chi}_1^0) \approx 5 : 1 : 0.2$.

5 Conclusions

In this note, we have extended the study of third family squarks in MSSM with complex parameters in Ref. [6] taking into account the cosmological bounds imposed by WMAP data. For this purpose, we have calculated numerically the decay widths of the third family superpartners $\tilde{t}_{1,2}$ and $\tilde{b}_{1,2}$, in particular, their dependences on the CP phase $\varphi_{U(1)}$. We have found that some decay channels like $\tilde{t}_2 \rightarrow b\tilde{\chi}_1^+$, $\tilde{t}_2 \rightarrow b\tilde{\chi}_2^+$, $\tilde{t}_2 \rightarrow t\tilde{\chi}_1^0$, $\tilde{t}_1 \rightarrow b\tilde{\chi}_1^+$, $\tilde{b}_1 \rightarrow t\tilde{\chi}_1^-$, $\tilde{b}_1 \rightarrow b\tilde{\chi}_1^0$, $\tilde{b}_2 \rightarrow t\tilde{\chi}_1^-$ and $\tilde{b}_2 \rightarrow t\tilde{\chi}_2^-$ show considerable dependences on $\varphi_{U(1)}$ phase. These decay modes will be observable at the LHC. Therefore they provide viable probes of CP violation beyond the simple CKM framework; moreover, they carry important information about the mechanism that brakes Supersymmetry.

The HEP community eagerly waiting the discovery of superpartners at the LHC. The obvious task in this context is to recognize them, for example via their spins, experimentally. There has been several studies in this direction [9,10]. Recently, Wang and Yavin [11] have studied in detail the possibility of measuring the spin of new particles in a variety of cascade decays, especially in the decay channel $\tilde{q} \rightarrow q\tilde{\chi}^\pm(\chi^0)$ which we consider here, and they conclude that the prospects for spin determination are rather good.

Acknowledgment

We would like to thank Durmus Ali Demir for suggesting the problem and valuable comments.

References

- [1] H. P. Nilles, Phys. Rep. **110** (1984) 1;
H. E. Haber and G. L. Kane, Phys. Rep. **117** (1985) 75;
R. Barbieri, Riv. Nuovo Cim. **11** (1988) 1;
J. F. Gunion and H. E. Haber, Nucl. Phys. B **272** (1986) 1 [Erratum-ibid. B **402** (1993) 567]; Nucl. Phys. B **278** (1986) 449
- [2] A. Pilaftsis, Phys. Lett. B **435** (1998) 88 [arXiv:hep-ph/9805373]. D. A. Demir, Phys. Lett. B **465** (1999) 177 [arXiv:hep-ph/9809360]; Phys. Rev. D **60** (1999) 055006 [arXiv:hep-ph/9901389]; A. Pilaftsis and C. E. M. Wagner, Nucl. Phys. B **553** (1999) 3 [arXiv:hep-ph/9902371].
- [3] D. A. Demir and K. A. Olive, Phys. Rev. D **65** (2002) 034007 [arXiv:hep-ph/0107329]; P. Gambino, U. Haisch and M. Misiak, Phys. Rev. Lett. **94** (2005) 061803 [arXiv:hep-ph/0410155]; M. E. Gomez, T. Ibrahim, P. Nath and S. Skadhauge, Phys. Rev. D **74** (2006) 015015 [arXiv:hep-ph/0601163]; G. Degrassi, P. Gambino and P. Slavich, Phys. Lett. B **635** (2006) 335 [arXiv:hep-ph/0601135].
- [4] D. N. Spergel, L. Verde, H. V. Peiris, E. Komatsu, M. R. Nolta, C. L. Bennett, M. Halpern, G. Hinshaw, N. Jarosik, A. Kogut, M. Limon, S. S. Meyer, L. Page, G. S. Tucker, J. L. Weiland, E. Wollack, E. L. Wright, Astrophys. J. Suppl **148** (2003) 175[arXiv:astro-ph/0302209];
C. L. Bennett, M. Halpern, G. Hinshaw, N. Jarosik, A. Kogut, M. Limon, S. S. Meyer, L. Page, D. N. Spergel, G. S. Tucker, E. Wollack, E. L. Wright, C. Barnes, M. R. Greason, R. S. Hill, E. Komatsu, M. R. Nolta, N. Odegard, H. V. Peiris, L. Verde, J. L. Weiland, Astrophys. J. Suppl **148** (2003) 1[arXiv:astro-ph/0302207];
- [5] G. Bélanger, F. Boudjema, S. Kraml, A. Pukhov, A. Semenov, Phys. Rev. D **73** (2006) 115007[arXiv:hep-ph/0604150];
- [6] A. Bartl, S. Hesselbach, K. Hidaka, T. Kernreiter, W. Porod, Phys. Rev. D **70** (2004) 035003[arXiv:hep-ph/0311338];

- [7] D. Chang, W. Y. Keung and A. Pilaftsis, Phys. Rev. Lett. **82** (1999) 900 [Erratum-
 ibid. **83** (1999) 3972] [arXiv:hep-ph/9811202]; S. Abel, S. Khalil and O. Lebedev,
 Nucl. Phys. B **606** (2001) 151 [arXiv:hep-ph/0103320]; D. A. Demir, M. Pospelov
 and A. Ritz, Phys. Rev. D **67** (2003) 015007 [arXiv:hep-ph/0208257]; D. A. Demir,
 O. Lebedev, K. A. Olive, M. Pospelov and A. Ritz, Nucl. Phys. B **680** (2004)
 339 [arXiv:hep-ph/0311314]; M. Pospelov and A. Ritz, Annals Phys. **318** (2005)
 119 [arXiv:hep-ph/0504231]; D. A. Demir and Y. Farzan, JHEP **0510** (2005) 068
 [arXiv:hep-ph/0508236].
- [8] J. S. Hagelin, S. Kelley and T. Tanaka, Nucl. Phys. B **415** (1994) 293; D. A. Demir,
 Phys. Lett. B **571** (2003) 193 [arXiv:hep-ph/0303249]; J. Foster, K. i. Okumura and
 L. Roszkowski, JHEP **0603** (2006) 044 [arXiv:hep-ph/0510422].
- [9] S. Abdullin *et al.* [CMS Collaboration], J. Phys. G **28** (2002) 469
 [arXiv:hep-ph/9806366].
- [10] J. Hisano, K. Kawagoe and M. M. Nojiri, squarks at Phys. Rev. D **68** (2003) 035007
 [arXiv:hep-ph/0304214].
- [11] L. T. Wang and I. Yavin, [arXiv:hep-ph/0605296].

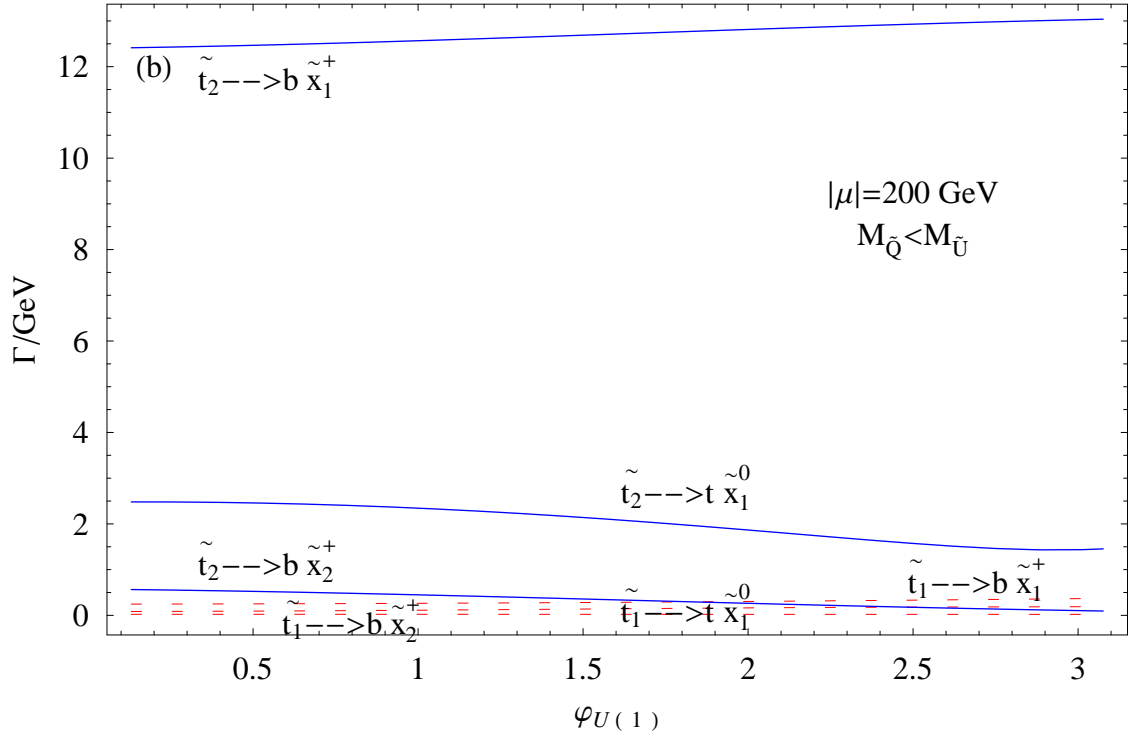
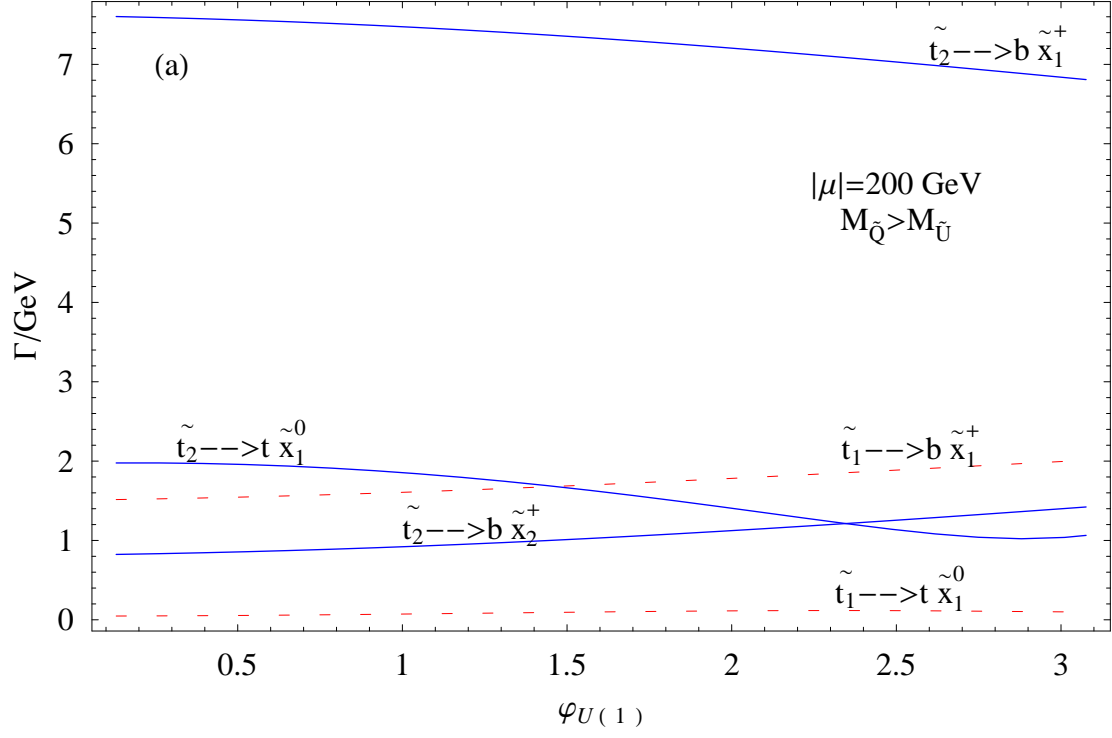


Figure 1: (a)-(b) Partial decay widths Γ of the $\tilde{t}_{1,2}$ decays for $\mu = 200 \text{ GeV}$, $\tan \beta = 10$, $A_t = 1.2 \text{ TeV}$, $\varphi_\mu = \varphi_{A_t} = 0$, $m_{\tilde{t}_1} = 350 \text{ GeV}$ and $m_{\tilde{t}_2} = 800 \text{ GeV}$.

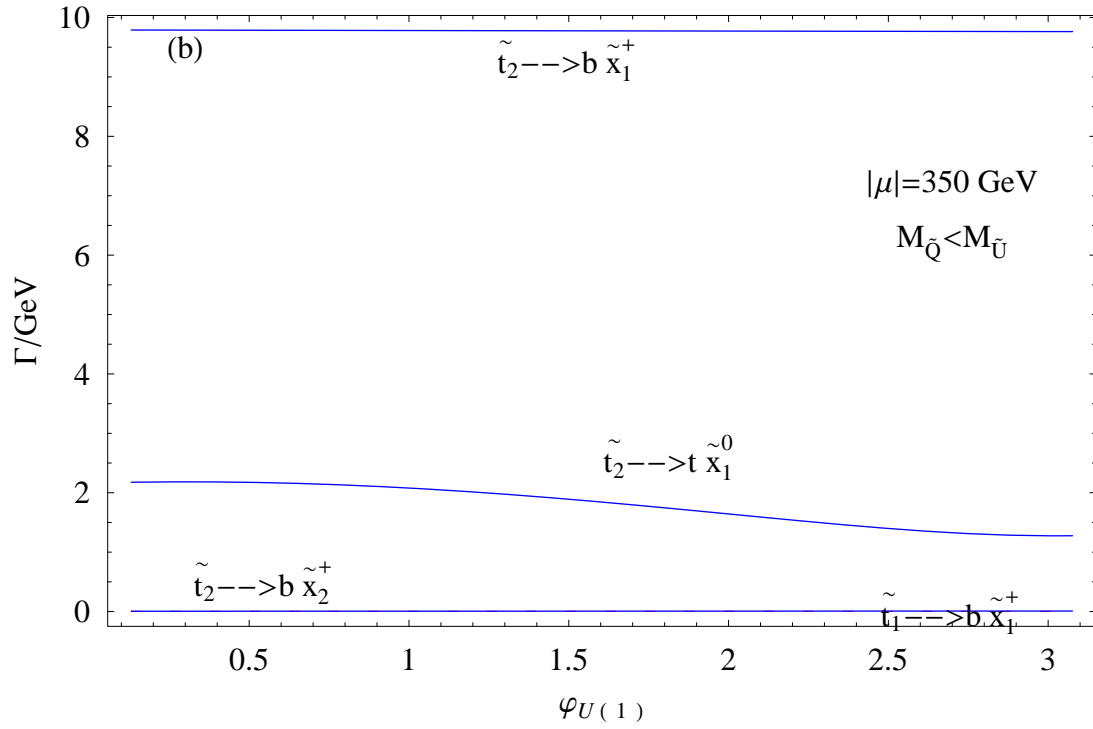
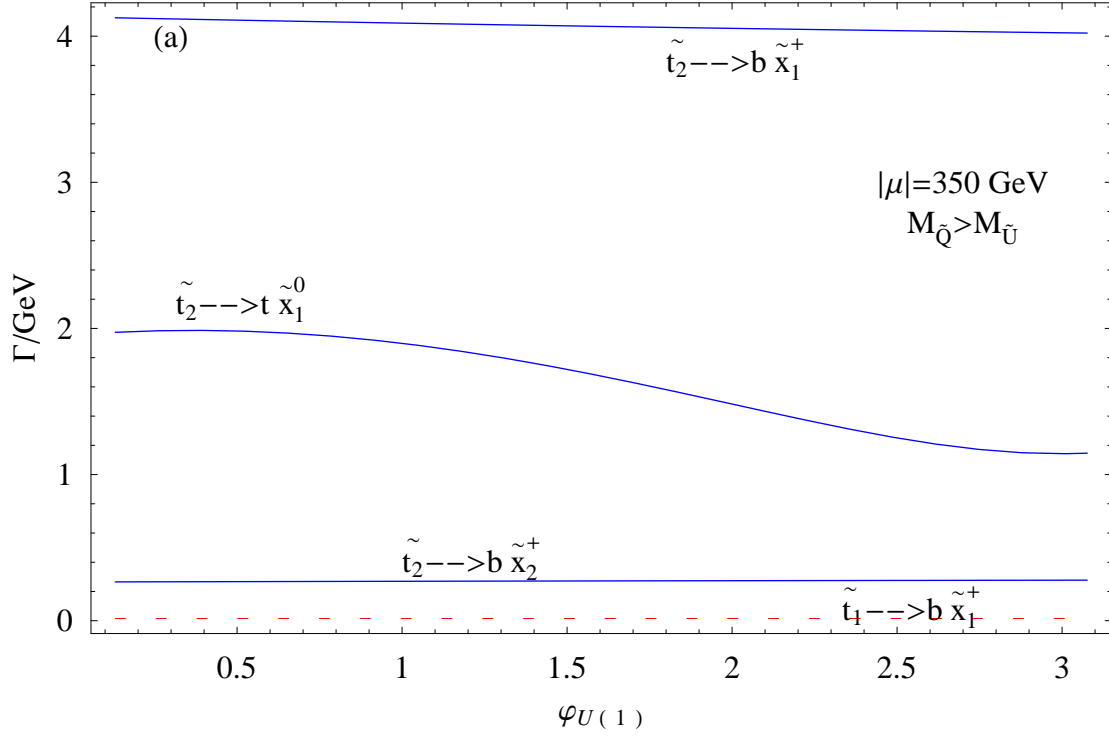


Figure 2: (a)-(b) Partial decay widths Γ of the $\tilde{t}_{1,2}$ decays for $\mu = 350 \text{ GeV}$, $\tan \beta = 10$, $A_t = 1.2 \text{ TeV}$, $\varphi_\mu = \varphi_{A_t} = 0$, $m_{\tilde{t}_1} = 350 \text{ GeV}$ and $m_{\tilde{t}_2} = 800 \text{ GeV}$.

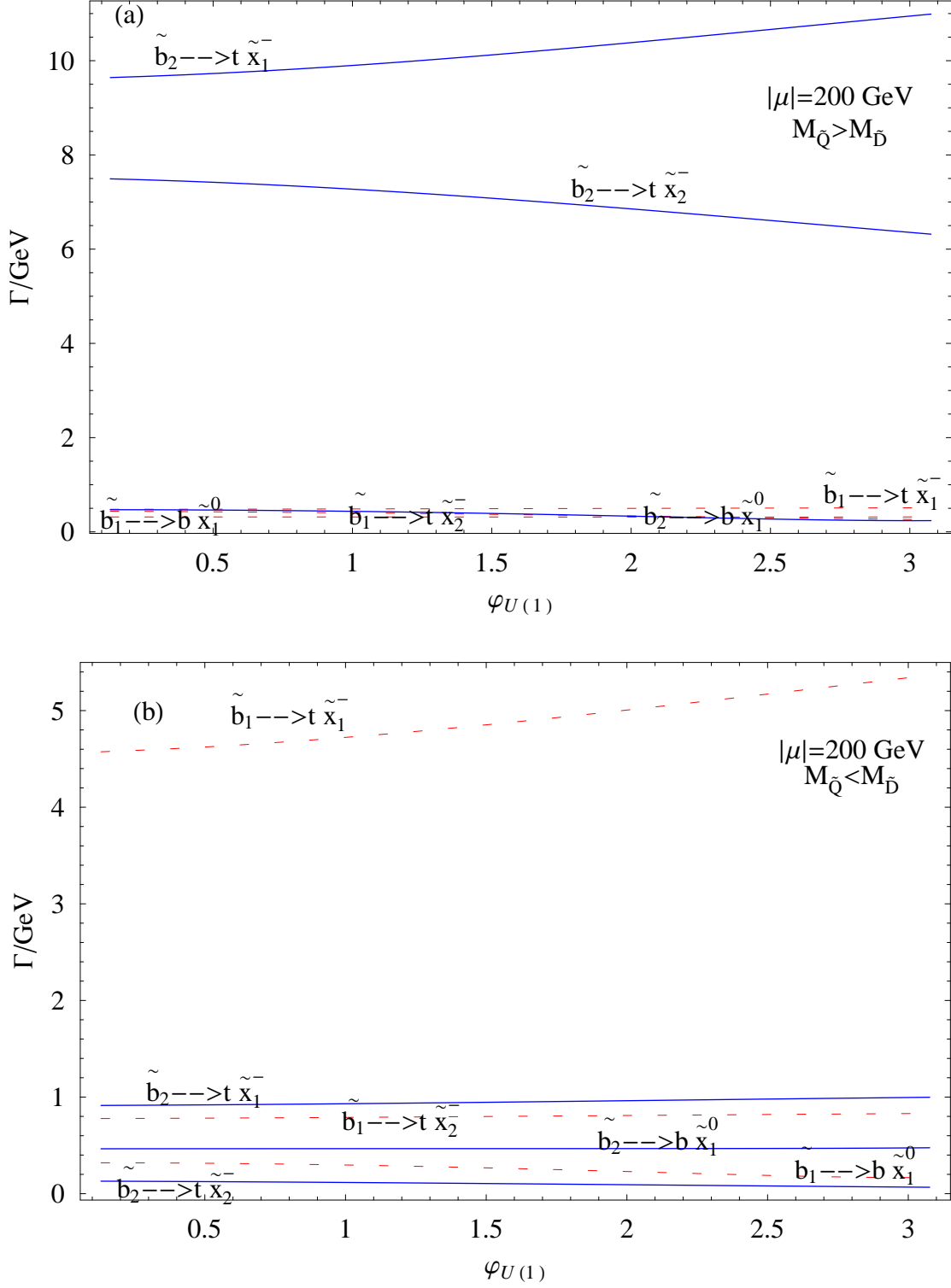


Figure 3: (a)-(b) Partial decay widths Γ of the $\tilde{b}_{1,2}$ decays for $\mu = 200$ GeV, $\tan \beta = 10$, $A_b = 1.2$ TeV, $\varphi_\mu = \varphi_{A_b} = 0$, $m_{\tilde{b}_1} = 550$ GeV and $m_{\tilde{b}_2} = 800$ GeV.

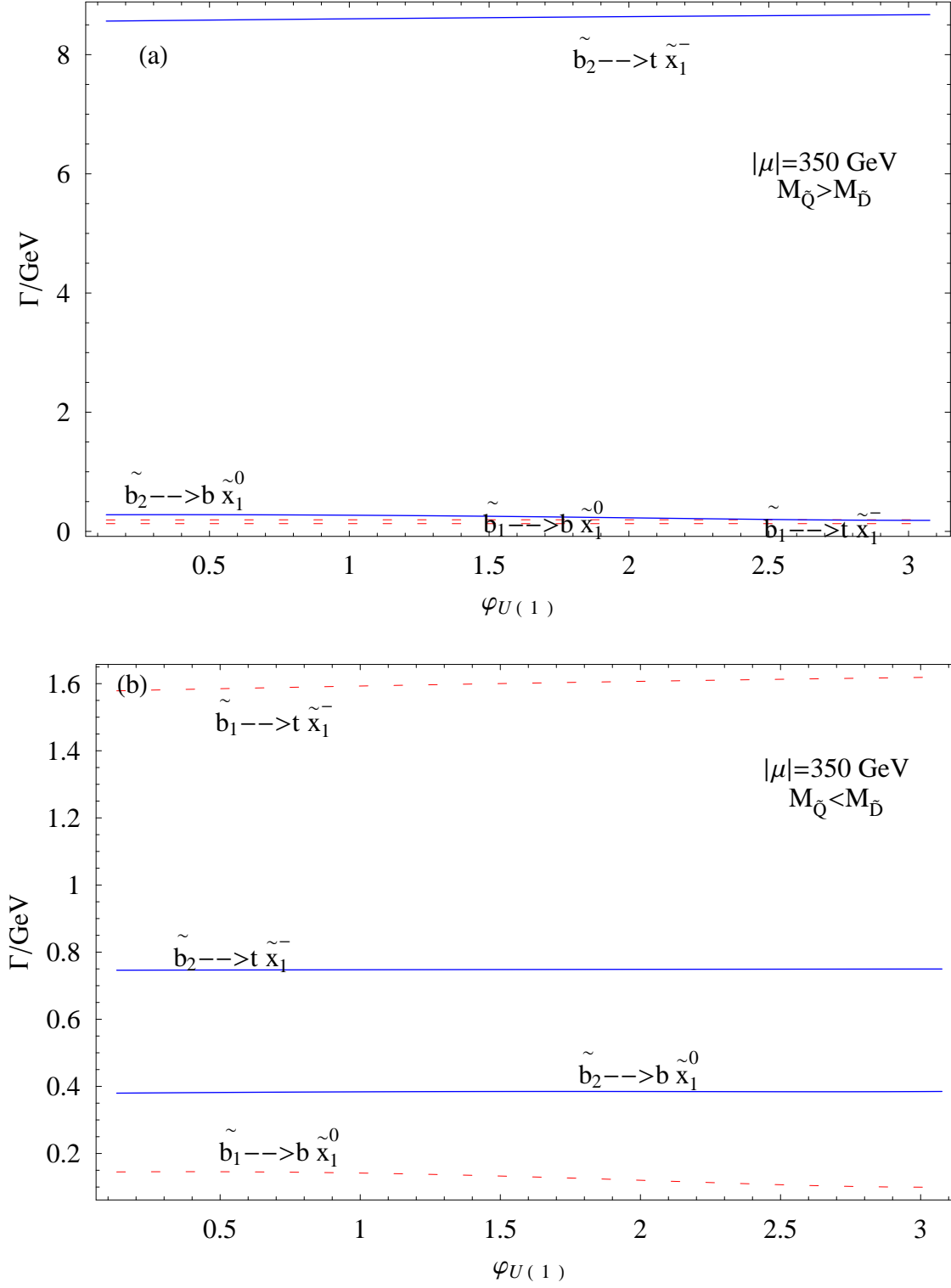


Figure 4: (a)-(b) Partial decay widths Γ of the $\tilde{b}_{1,2}$ decays for $\mu = 350$ GeV, $\tan \beta = 10$, $A_b = 1.2$ TeV, $\varphi_\mu = \varphi_{A_b} = 0$, $m_{\tilde{b}_1} = 550$ GeV and $m_{\tilde{b}_2} = 800$ GeV.

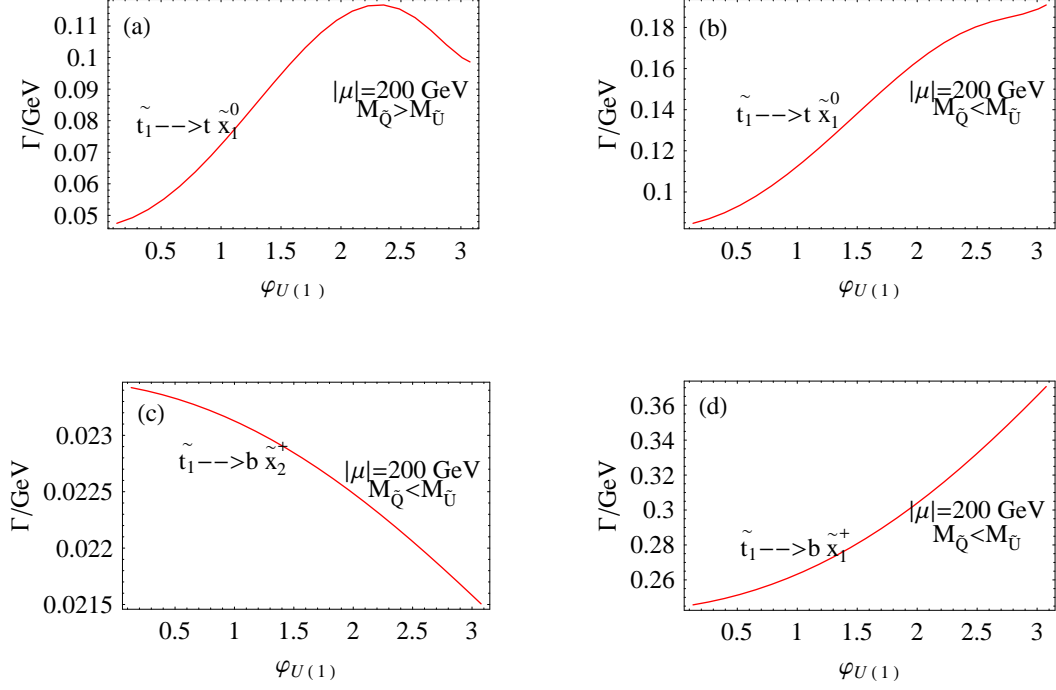


Figure 5: (a)-(d) $\varphi_{U(1)}$ dependences of certain $\tilde{t}_{1,2}$ decays for $\mu = 200 \text{ GeV}$.

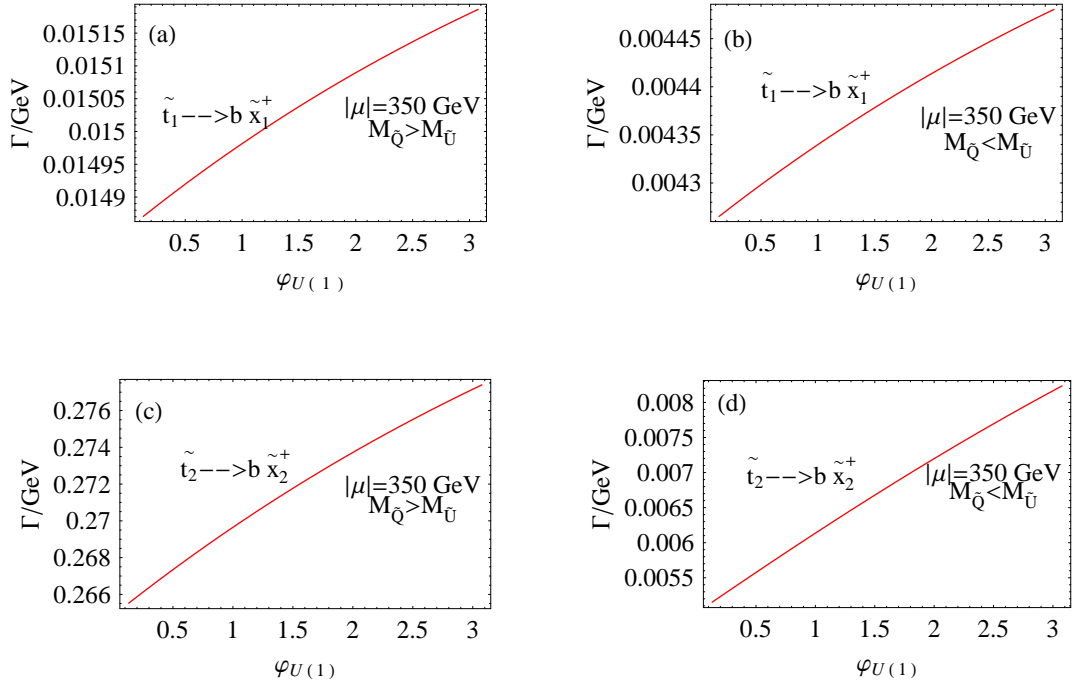


Figure 6: (a)-(d) $\varphi_{U(1)}$ dependences of certain $\tilde{t}_{1,2}$ decays for $\mu = 350 \text{ GeV}$.

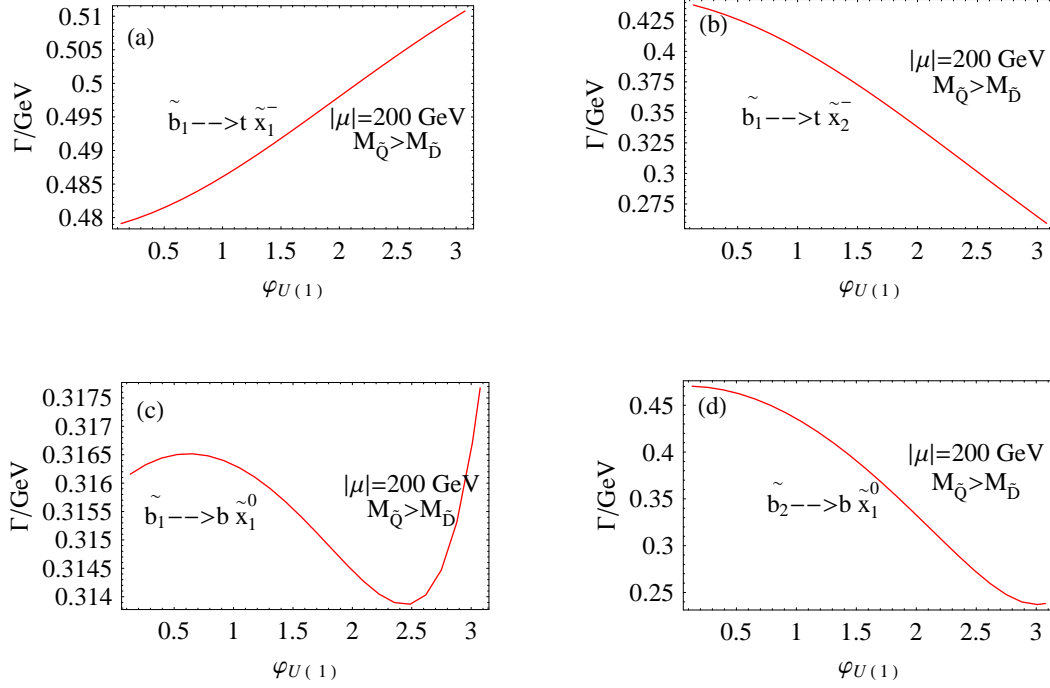


Figure 7: (a)-(d) $\phi_{U(1)}$ dependences of certain $\tilde{b}_{1,2}$ decays for $\mu = 200 \text{ GeV}$.

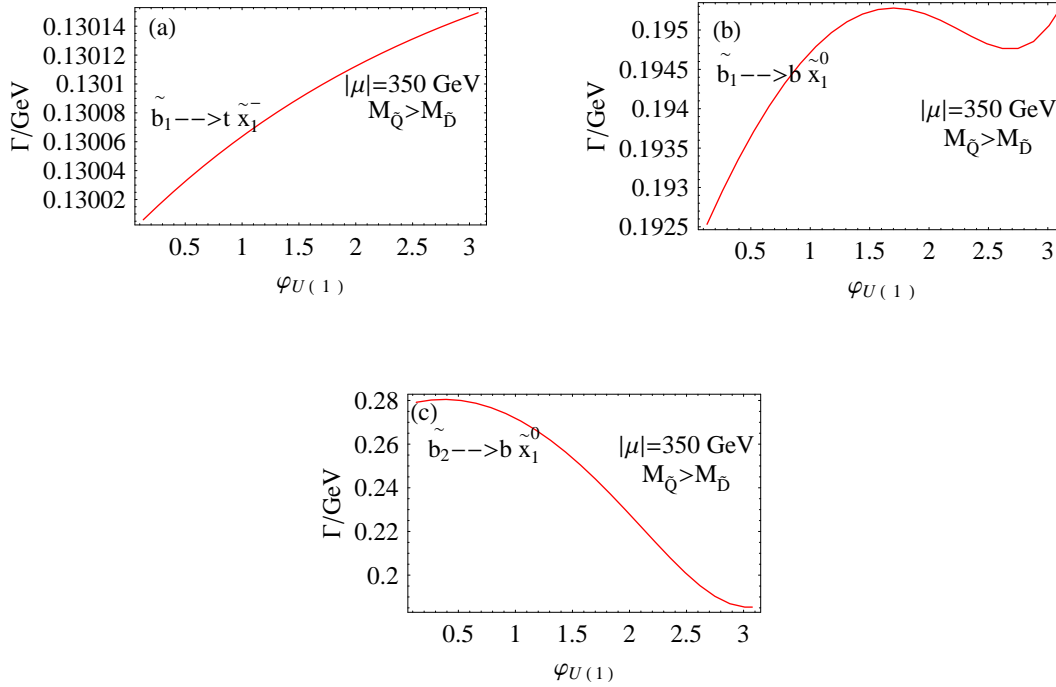


Figure 8: (a)-(d) $\phi_{U(1)}$ dependences of certain $\tilde{b}_{1,2}$ decays for $\mu = 350 \text{ GeV}$.